

Analysis of transpiration results from the RICE and PILPS Workshop

J.-F. Mahfouf ^{a,*}, C. Ciret ^b, A. Ducharne ^c, P. Irannejad ^b, J. Noilhan ^a, Y. Shao ^b,
P. Thornton ^d, Y. Xue ^e, Z.-L. Yang ^f

^a METEO-FRANCE, CNRM, Toulouse, France

^b Climatic Impacts Centre, Macquarie University, Sydney, Australia

^c LMD / CNRS, Rue Lhomond, Paris, France

^d NTSG, School of Forestry, University of Montana, Missoula, USA

^e COLA, Department of Meteorology, College Park, Maryland, USA

^f Institute of Atmospheric Physics, University of Arizona, Tucson, USA

Received 5 May 1995; accepted 28 August 1995

Abstract

Results from the 14 land surface parameterization schemes involved in the PILPS–RICE Workshop are compared for a soya crop growing season (from June to September). During this period, the transpiration flux dominates the total surface evapotranspiration and observed data from HAPEX–MOBILHY are available for comparison. Results indicate that during the month of June half of the models fall within the uncertainty range of the observations.

The scatter between models behaviour is explained by three major reasons:

- The functional dependency between soil moisture and transpiration;
- the initial moisture content at the beginning of the period;
- the vertical discretization within the soil and the extension of the root system that defines the soil water holding capacity for plants

Examination of diurnal cycles of evaporation reveals that formulations based on the supply–demand concept are very sensitive to the specification of the root zone.

This analysis underlines the need for more sensitivity experiments to be done with the current forcing data set and more detailed datasets to be collected in future field experiments (e.g. latent heat flux during all the growing season, root zone distribution).

1. Introduction

The main goal of the RICE and PILPS Workshop was to evaluate soil moisture simulations in current land surface parameterization schemes developed for

atmospheric, hydrological and ecological purposes. All these disciplines need an accurate estimation of the surface water budget over continental surfaces. Soil moisture is a key parameter controlling this budget and strongly influences the other components. Soil moisture availability controls the flux of water vapour leaving the surface through soil pores and plant stomata. The water holding capacity of a soil

* E.C.M.W.F., Shinfield Park, Reading, Berkshire RG2 9AX, UK. E-mail: paf@ecmwf.int.

determines to a large extent the partition of incident precipitation between storage and runoff. All these statements imply that the evolution of soil moisture has to be accurate enough over the time scales of interest (from one month to several years for climatic purposes). Land surface schemes have also to provide a sound link between soil moisture and water fluxes directly affecting the lower atmosphere (surface evapotranspiration) and the deep ground hydrology (runoff and drainage).

The purpose of this paper is to present and analyze results obtained from this intercomparison during the summertime period where surface evapotranspiration is dominated by plant transpiration. The general framework of this comparison is described in Shao et al. (1995) and will not be repeated here. With respect to other aspects of land surface schemes examined in companion papers (Desborough et al., 1996-this issue; Wetzel et al., 1996-this issue), plant transpiration is certainly more difficult to simulate. Runoff and bare soil evaporation are based on well-defined physical concepts (water transfers in porous media) even though they are strongly non-linear inducing large spatial heterogeneities. On the contrary, the processes and mechanisms controlling transpiration are more complicated, involving the interaction of abiotic factors (such as pressure–volume characteristics of the soil, the radiation environment, and leaf boundary layer dynamics) with biotic factors (such as diffusion of water across root membranes, transport in the liquid phase through the conductive tissue, and biochemical signals controlling stomata). Simplifying assumptions are required in order to represent this system numerically, and much of the variation between schemes is due to different simplifications. This is true of all numerical implementations of natural processes, but the interaction of biotic and abiotic factors that characterizes this particularly complex system requires a wider range of simplifications than in the case of evaporation from bare soil.

Two original aspects of the results obtained during this Workshop concerning plant transpiration can be outlined:

- The HAPEX–MOBILHY dataset has provided measurements of all the components of the surface water budget during a one month period (Intensive Observing Period: IOP) associated with

the beginning of the growing phase of a soya crop. Precipitation and soil moisture have been measured during one year, allowing a partial examination of the surface water budget during the entire growing cycle of the crop.

- The wide variety of surface schemes has enabled the comparison of the most currently used formulations of plant transpiration.

In section 2 we describe the various approaches developed so far in land surface schemes to represent plant transpiration. They are based on physical and physiological understanding of the processes involved. Section 3 focuses on the analysis of the results during both the IOP (one month) and the growing season (four months). Conclusions are provided in the last section together with needs and strategies for future intercomparisons of land surface schemes against observed datasets.

2. Parametrization of transpiration

2.1. General features

Transpiration is a physiological process associated with photosynthesis, which involves the transfer of water from soil through the roots, stems, branches and leaves. In most landsurface schemes, the parameterisation of transpiration is achieved by introducing the concept of canopy resistance as a measure of the control of moisture transfer by the vegetation (Monteith, 1965).

For fully vegetated surfaces, the transpiration flux is described by

$$E_{tr} = \rho(q_{sat}(T_c) - q_a)/(r_a + r_c) \quad (1)$$

with r_c being the bulk stomatal resistance or bulk canopy resistance, and r_a an aerodynamic resistance described by Monin-Obukhov similarity theory (Stull, 1988).

Bulk stomatal resistance is a sub-grid scale variable and is difficult to measure. In most of the landsurface schemes, the stomatal resistance of a leaf, R_{st} is calculated and the bulk stomatal resistance r_c is obtained by assuming all the leaves of the canopy to operate in parallel using an analogue of Ohm's law. A common assumption is that

$$r_c = R_{st}/LAI \quad (2)$$

where LAI is the leaf area index.

R_{st} is expressed as a function of minimum leaf stomatal resistance R_{smin} and of external factors to represent photosynthetic activity and the limitation of water losses by the plant in unfavorable environmental conditions (soil moisture availability, atmospheric water vapour deficit, solar radiation, air temperature and carbon-dioxide concentration). The difficulty of this approach is to use functional dependencies suitable for a wide range of vegetation types. The proposal of Jarvis (1976), where R_{st} is expressed as a product of independent factors, is often adopted.

Another approach to represent the reduction of transpiration flux in unfavorable environmental conditions was introduced by Federer (1979, 1982). Transpiration is limited by the supply of water from the roots or by the atmospheric demand (mostly driven by radiation). The maximum water flux that the plant can supply for a given soil moisture content is compared to the water flux in unstressed conditions, the minimum of these two quantities is then chosen (Wetzel and Chang, 1987).

2.2. Summary of the various approaches

The formulation of the basic equations used represent evaporative fluxes from vegetation varies among the models represented at the Workshop. Some of this variation is due to fundamental structural differ-

ences between models, such as different time-steps (from minute to one day) or different soil layer structures (from one to nine layers), and some of the variation is due to differences in the conceptualization of the transpiration process in the models.

Attention was focussed on the representation of one element of this system, the control of evapotranspiration by soil moisture. This seemed the most relevant aspect of the entire system to the overall goals of the Workshop, and one that would give us a first glimpse at the more fundamental differences between schemes. It is a necessary step in the process towards understanding, but it is far from sufficient.

Table 1 summarizes the main features of each scheme related to the representation of water transfers from the root zone to the atmosphere. The second column gives a brief description of the general transpiration formulation employed by the schemes. There appear to be two distinct categories: those schemes that assess transpiration as the minimum of a supply function and a demand function, and include the influence of soil moisture in their supply equations (*S&D*); and those schemes that use some derivative of an Ohm's law model (r_c), and include the influence of soil moisture as a change in canopy resistance or moisture availability (so-called β -parameter). Relationships between soil moisture and transpiration are depicted in Table 2. There is a

Table 1

Summary of the representation of transpiration. *S&D* corresponds to the supply–demand approach, r_c to representations based on the canopy surface resistance concept, and β to representations using the moisture availability concept (ratio of actual to potential evaporations)

Model	Timestep	Transpiration formulation	Number of soil layers	Depth of effective root zone (cm)
BATS	30 min	<i>S&D</i>	3	50
BEST	30 min	<i>S&D</i>	2	150
BGC	1 day	r_c	3	50
BIOME2	1 day	<i>S&D</i>	2	50
BUCKETP	30 min	β	1	160
CENTURY	1 day	β	9	50
CLASS	30 min	r_c	3	50
CSIRO9	30 min	r_c	2	160
ISBA	30 min	r_c	2	160
LAPS	30 min	r_c	3	50
PLACE	30 min	<i>S&D</i>	7	50
SECHIBA2	30 min	β , r_c	2	160
SSiB	30 min	r_c	3	50
VIC	60 min	r_c	2	50

wide range of implementations, from simple ratios to exponential and power relationships, having varying numbers of parameters that specify the shapes of the functions. In the second group the shape of the relationships between soil moisture and canopy resistance are different, but also some empirical parameters such as the minimum stomatal resistance, or the threshold when water stress begins and transpiration ceases. Values of these parameters are also reported in Table 2 as they explain some differences in model behaviour.

Fig. 1 represents the evolution of the ratio of transpiration E_{tr} to potential evaporation E_{pot} (hereafter defined as moisture availability) with soil

water content, as given by the schemes based on canopy resistance and moisture availability concepts. The atmospheric resistance r_a is set to an arbitrary value of 50 s/m to allow comparison between the two formulations. Indeed, the equivalent moisture availability of schemes including a canopy resistance can be written:

$$\beta = \frac{r_a}{r_a + r_c}$$

For most of the schemes, transpiration is negligible below the wilting point, except for CLASS. During the Workshop, participants agreed on same set of textural soil properties and definitions of wilt-

Table 2

Summary of the parameterisation of transpiration. W is the volumetric water content over the root zone, W_{wilt} is the volumetric water content at wilting point and W_{fc} the volumetric water content at field capacity. Ψ is the matrix water potential, Ψ_{sat} is the matrix water potential at saturation, and Ψ_{wilt} is the matrix water potential at wilting point

Model	Relation with soil moisture	Parameters
BATS	$f\left(\frac{\Psi - \Psi_{wilt}}{\Psi_{sat} - \Psi_{wilt}}\right)$	$R_{sm\,in} = 40 \text{ s/m}$
BEST	$S = E_{tmax} \left[1 - \left(\frac{W_{wilt}}{W} \right)^b \right], D = D(R_s)$	$R_{sm\,in} = 150 \text{ s/m}$
BGC	$\frac{\Psi - \Psi_{wilt}}{\Psi_{sat} - \Psi_{wilt}}$	$R_{sm\,in} = 100 \text{ s/m}$
BIOME2	$\beta = \frac{W - W_{wilt}}{W_{fc} - W_{wilt}}, S = c_1 \beta$	$c_1 = 1 \text{ mm/hr}$
BUCKETP	$\beta = \frac{W - W_{wilt}}{0.75(W_{fc} - W_{wilt})}$	
CENTURY	$\beta = \beta(\Psi)$	
CLASS	$\max\left(1, \frac{\Psi}{\Psi_{wilt}}\right)$	$R_{sm\,in}/LAI = 50 \text{ s/m}, \Psi_{wilt} = 150 \text{ m}$
CSIRO9	$\frac{W - W_{wilt}}{0.75W_{sat} - W_{wilt}}$	$R_{sm\,in} = 50 \text{ s/m}$
ISBA	$\frac{W - W_{wilt}}{W_{fc} - W_{wilt}}$	$R_{sm\,in} = 200 \text{ s/m}$
LAPS	$\left[1 - \left(\frac{W_{wilt}}{W} \right)^{1.5} \right]^{-1}$	$R_{sm\,in} = 40 \text{ s/m}$
PLACE	$\dot{S} = \Psi_{wilt} - \frac{\Psi_{soil}}{r_s(K)} + r_p, D = \rho C_D U_a \frac{q_{sat} - q_a}{r_a + r_e + r_c}$	$R_{sm\,in} = 150 \text{ s/m}$
SECHIBA2	$\beta = \frac{r_a}{r_a + r_s + r_0} \exp\left(-c \frac{W_{fc} - W}{W_{fc} - W_{wilt}}\right)$	$R_{sm\,in} = 77 \text{ s/m}, c = 0.8$
SSiB	$1 - \exp[-c_2(c_1 - \ln(-\Psi))]$	$R_{sm\,in} = 117 \text{ s/m}, c_2 = 1.7, c_1 = \ln(-15 \text{ bar})$
VIC	$\frac{W - W_{wilt}}{0.70W_{fc} - W_{wilt}}$	$R_{sm\,in} = 40 \text{ s/m}$

ing point and field capacity on the basis of the Clapp and Hornberger (1978) and Cosby et al. (1984) data sets. This explains why the strong decrease of moisture availability below the wilting point ($0.15 \text{ m}^3 \text{ m}^{-3}$) is coherent between the schemes. The starting point for hydric stress is very different between the schemes. For SSiB, the dependence of transpiration with soil moisture takes place in a very sharp region close from the wilting point. This comes from a dependency of the stress function with water potential, whereas most of the schemes have a dependency with volumetric water content. By contrast, schemes like ISBA or LAPS have a wider range of variation of transpiration with soil moisture. Schemes with high values of E_{tr}/E_{pot} for wet soils are expected to evaporate strongly at the beginning of the growing period (BUCKETP, VIC, SSiB). Schemes with a rapid decrease of E_{tr}/E_{pot} with soil moisture will tend to produce contrasted phases with high evaporation rates followed by much weaker ones. A smoother transition between potential evaporation and stressed transpiration regimes is expected from schemes like ISBA, LAPS or CSIRO9. The functional dependency of the stress function in SECHIBA2 leads to a

discontinuity at wilting point. A discontinuity is also observed for LAPS at field capacity.

When the soil is above field capacity ($0.32 \text{ m}^3 \text{ m}^{-3}$), the level of the plateau of the various curves is explained by the choice of the minimum (unstressed) stomatal resistance (indeed in that range, $\beta = r_a / [r_a + R_{smin}/LAI]$). For example, CSIRO9 and ISBA, although having the same functional dependency with soil moisture, have specified R_{smin} values of 50 s/m and 200 s/m, respectively.

Another aspect of the theory and numerical implementation of the various schemes is the dependence of the soil moisture/canopy resistance relationship on the structural definition of the soil layers and the treatment of root distribution in those layers. The various schemes use differently the root proportion information specified as a site parameter in the assessment of soil moisture stress at different levels in the soil. Schemes resolving the first 50 cm of soil extract soil moisture for transpiration mostly from this layer (CENTURY, VIC, PLACE, BATS, BIOME2, CLASS, BGC, SSiB, LAPS) whereas those having a bulk reservoir in the root zone have a much higher water holding capacity (ISBA, CSIRO9,

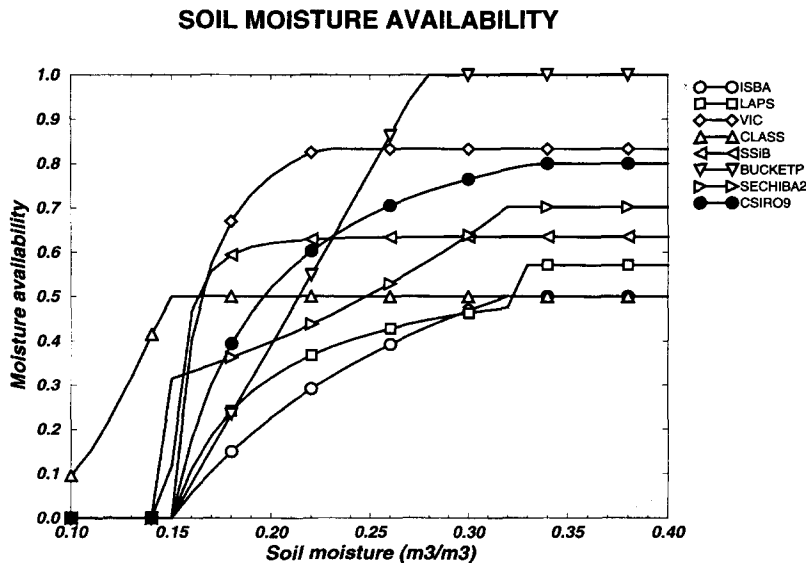


Fig. 1. Evolution of the soil moisture availability with soil moisture content for a fully covered canopy for eight land surface schemes. Soil moisture availability β is defined as the ratio of actual evapotranspiration to potential evapotranspiration E_{pot} ($E = \beta E_{pot}$). A constant aerodynamic resistance of 50 s/m is assumed when expressing schemes based on canopy resistance concept in terms of moisture availability.

BUCKETP, SECHIBA2, BEST) as summarized in Table 1. The reason is that they implicitly distribute the roots within the whole profile (1.6 m). We will see in the results that important differences between schemes responses come from fundamental differences in soil water stress response.

In summary, while the brief initial investigation of the theory and numerical implementation of the transpiration fluxes in participating schemes revealed some similar approaches with quite disparate implementations, the sensitivity of the schemes to the exact formulations employed has yet to be demonstrated. A thorough understanding of the differences in behaviour between schemes will require an examination not only of the equations used to calculate the transpiration fluxes, but also of the interaction of the calculated fluxes with the logical structuring of soil layers and root distribution.

3. Design of the experiments

The design of experiments undertaken during the Workshop is fully described in Shao and Henderson-Sellers (1996-this issue), so only a summary is given here. The land surface schemes are forced by a time series of near-surface atmospheric and radiative parameters, and precipitation measured at the Caumont site (southwestern France) during the HAPEX–MOBILHY 1986 field campaign (André et al., 1988). The sampling of the atmospheric forcing is 30 minutes. The data set starts on 1st January and lasts for one year. The site was a soya crop field with vegetation during five months (May to September) and bare soil during other times. Various experiments were performed during the Workshop corresponding to different soil and vegetation parameters that were not measured during HAPEX–MOBILHY (Shao and Henderson-Sellers, 1996-this issue).

In Experiment 13 which is analyzed here, schemes were forced with the same meteorological data and had the same prescriptions for soil characteristics (Cosby et al., 1984) and vegetation structure. Each scheme was allowed to come to equilibrium with the atmospheric forcing data and establish its own annual pattern of moisture and energy fluxes. It was hoped to reach some general conclusions about differences between schemes by analyzing their be-

haviour in a 'native' or 'operational' mode. Another incentive to study these results was the availability of observations during the forcing period against which the control experiment results could be compared or validated.

Two independent observation data sets were used as references in the comparison of the simulated latent heat fluxes and soil water changes during the growing period. One set of observations consisted of measurements of net radiation, sensible heat flux, and ground heat flux on 15 minute intervals, for a period of 37 days, with complete observations from day 148 (28 May 1986) through day 184 (3 July 1986) during the IOP of HAPEX–MOBILHY. Estimates of latent heat fluxes based on these measurements were derived as the residual of the energy budget equation (Goutorbe, 1991; Goutorbe and Tarrieu, 1991). The other set of observations consisted of the precipitation data, measured at the site every 15 minutes, and weekly measurements of soil water content at several depths. Estimates of evaporative fluxes were derived from these observations based

Table 3

Water budget during the growing season. ΣE_{tot} is the accumulated total evaporation from day 148 to day 274 (expressed in mm). ΣE_g is the accumulated bare soil evaporation from day 148 to day 274 (expressed in mm). $m(1)$ is the water amount at the beginning of day 148 over the whole soil column (1.6 m). $m(2)$ is the water amount at the beginning of day 274 over the whole soil column (1.6 m). $\Delta m = m(1) - m(2)$, ΣP is the accumulated precipitation from day 148 to day 274 (177 mm) and R is the residual term of the water balance (a negative term is a loss for the soil column)

Model	ΣE_g	ΣE_{tot}	$m(1)$	$m(2)$	$\Delta m + \Sigma P$	R
BATS	58	272	469	371	275	-3
BEST	70	344	428	260	345	-1
BGC	50	306	483	349	311	-5
BIOME2	4	272	478	369	286	-14
BUCKETP	0	324	438	282	333	-9
CENTURY	10	249	453	355	275	-26
CLASS	85	310	450	295	332	-22
CSIRO9	87	387	586	373	390	-3
ISBA	108	341	477	315	339	2
LAPS	167	382	560	452	285	97
PLACE	37	316	436	302	311	5
SECHIBA2	10	381	495	292	380	1
SSiB	139	358	521	294	404	-46
VIC	31	287	518	351	344	-57
HAPEX	-	320	508	364	321	1

on the water budget equation, using the assumption that there was no runoff or drainage out of the 1.6 m soil column during this period. These estimates were only possible when there was a soil moisture measurement, and so they provide a fairly coarse means of evaluating fluxes at the site, although they do provide flux estimates for the whole of the growing season.

Results of the comparisons during the IOP are presented below, followed by results of comparisons throughout the growing season. The growing season has been chosen from 28 May to 30 September (4-month period) corresponding to the period where the crop has reached a mature stage so that the surface evaporation flux is dominated by the contribution of the vegetation. Although the soya crop begun to grow at the beginning of May, the amount of bare soil remains significant during that month. Including this period in the growing phase would lead to a more difficult interpretation of the results. The goal of the various groups formed during the Workshop was to select specific time periods in order to isolate processes (transpiration, bare soil evaporation, runoff) for a better understanding of the model behaviours. Table 3 reports cumulative total

evaporation and evaporation from bare ground simulated by all the schemes during the 4 summer months. It shows that vegetation evapotranspiration ranges from 60 to 100% of total evaporation. During that period the vegetation cover is set to a constant value of 90% and the leaf area index is equal to 4.

Discussion also includes an assessment of the coherence between these two independent observation data sets used to retrieve the surface evaporation flux (surface energy budget on one side and surface water budget on the other side).

Experiment 13 cannot be considered as the simulation that leads to the best agreement with observations (experiment 15 was designed for that but more modifications and tunings of the various schemes were allowed). Comparison of results with observed data will be done with caution, because the observed data present some inconsistencies. Observed evaporation estimated with atmospheric sensors is close to the residual between soil moisture estimates from neutron probes and precipitation measurements during the IOP (Mahfouf, 1990). The imbalance between these two quantities gives an indication on the accuracy of the total retrieved evaporation (25 mm for a total amount of 126 mm). Ideally observations

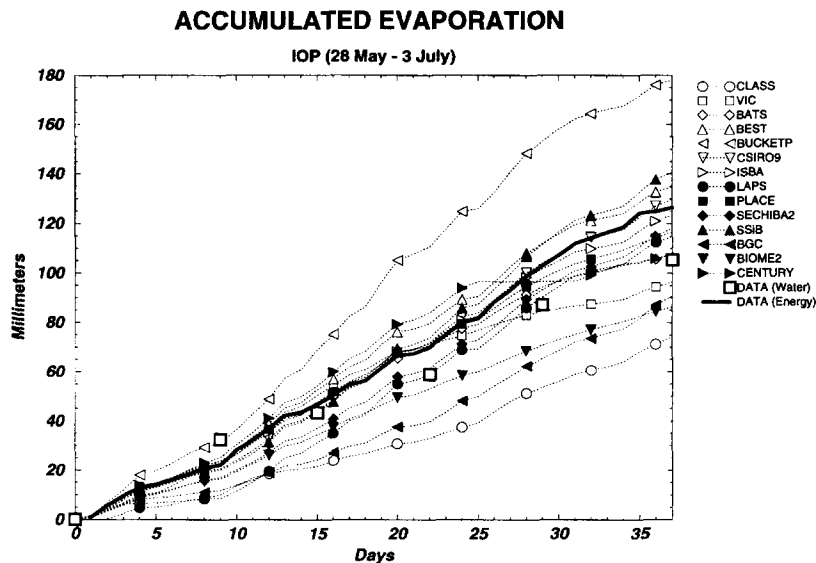


Fig. 2. Observed and predicted values of accumulated evaporation during the Intensive Observing Period (IOP) at the location of Caumont (from day 148 to day 184). The solid curve corresponds to the atmospheric measurement by the SAMER station (energy balance method) and the squares are weekly retrievals from the residual of the surface water balance (soil moisture and precipitation) assuming no drainage.

would also be required to set some of the input parameters of the landsurface schemes. We have tried to impose parameters defining the surface in a coherent manner, from the available observations. Unfortunately, most of the parameters characterizing the description of the soya crop were not measured (root density, *LAI*, vegetation cover). Other parameters like R_{min} depend on the scheme used and can hardly be imposed as a common value. For example, schemes having a dependency on vapour pressure deficit will impose a lower value for R_{min} to produce the same canopy resistance as schemes that do not account for this effect. Moreover, some participants have preferred to impose the parameters they use to choose for crop vegetations in their host model, rather than ones tuned for this specific dataset. The consequence is that the performance of such schemes can be poorer with respect to schemes having tuned parameters. This reveals that the differences seen below can also come from methodological choices.

4. Analysis of the control experiment

4.1. Intensive observing period (IOP) results

Estimates of evapotranspiration fluxes during the IOP derived from the residual of the energy budget equation for measured values of net radiation, sensible heat flux, and ground heat flux, give a total amount of 126 mm summed over 37 days, or an average flux of 3.40 mm/day. The accumulated mean daily evapotranspiration for all schemes is presented in Fig. 2 together with measurements from the SAMER station (solid line) and from neutron soundings and precipitation (open squares) assuming no runoff during this period. More than half of the models reproduce total evaporation close to these two estimates from the data (SSiB, SECHIBA2, BEST, CSIRO9, ISBA, PLACE, LAPS BATS).

Two models have a very different behaviour than observations. BUCKETP overestimates by 60 mm the evaporation and CLASS only evaporates 75 mm during the IOP. Fig. 1 explains such differences: BUCKETP evaporates at a potential rate when soil moisture is above $0.75 \times (w_{\text{fc}} - w_{\text{wilt}})$ which is the case at the beginning of the IOP. There is no control

of the water flux by the surface. During this period (June) the evaporative demand is high and explains simulated amounts by this scheme. This result is interesting because it shows that the observed evapotranspiration rate is significantly lower than the potential rate for unstressed vegetation.

On the other hand, control exerted by CLASS on transpiration appears excessive. R_{min}/LAI is set to 50 s/m which leads to $R_{\text{min}} = 200$ s/m with $LAI = 4$ as shown by the level of the plateau on curves displayed in Fig. 1. Since this value is the same as ISBA, which nevertheless produces much higher evaporation rates, we have to search for another reason to explain the difference. Accumulated bare soil evaporation over the IOP is much lower in CLASS than in ISBA (23 mm against 66 mm) although transpiration rates are similar (47 and 52 mm, respectively). Such a difference in bare soil evaporation is explained by the use of a separate energy budget for the soil surface in CLASS whereas ISBA has a single temperature for both soil and vegetation.

Some schemes simulate a total amount of evaporation close to observations but show compensating mismatches at the beginning and the end of the IOP. LAPS produces very low evaporation rates during the first 10 days that are compensated by higher evaporation rates afterwards. CENTURY has the largest evaporation rate after BUCKETP during the first 25 days followed by low rates until the end of the IOP. The VIC model has a similar behaviour: evaporation is close to observations up to day 25 and is thereafter strongly reduced. The main reason for this lies in the vertical structure of the roots within the soil layer that allows water to be extracted only in the first 50 cm. It induces a smaller water-holding capacity than for other schemes. The effect is evident for these two models (VIC and CENTURY) and not for others having the same structure because they lose soil water more rapidly. The VIC model allows a significant amount of gravitational drainage even in the summertime period, and the stress function is ineffective for CENTURY in the early stages of the IOP. Another feature of these two schemes is that transfer between layers only operates from top to bottom. The process of capillary rise that could moisten a dry superficial layer from wetter deep horizons is not simulated by these schemes.

Note that vertical structure alone is not enough to stratify model's behaviour, as illustrated by the following examples from two models which have the same vertical structure as VIC, namely roots in the top 50 cm of soil. BIOME2 has an insufficient total amount of evaporation, because of a constant underestimation for all regimes. The evaporation for SSiB is close to observations in the first 20 days, but

towards the end there is a tendency for over-evaporation due to the rather flat shape of the evaporative stress function (Fig. 1).

Of the 14 schemes involved in the intercomparison, only three of them do not resolve the diurnal cycle (the ecological models BIOME2, BGC and CENTURY). For the others it is important to check their behaviour at the daily time scale. Most of the

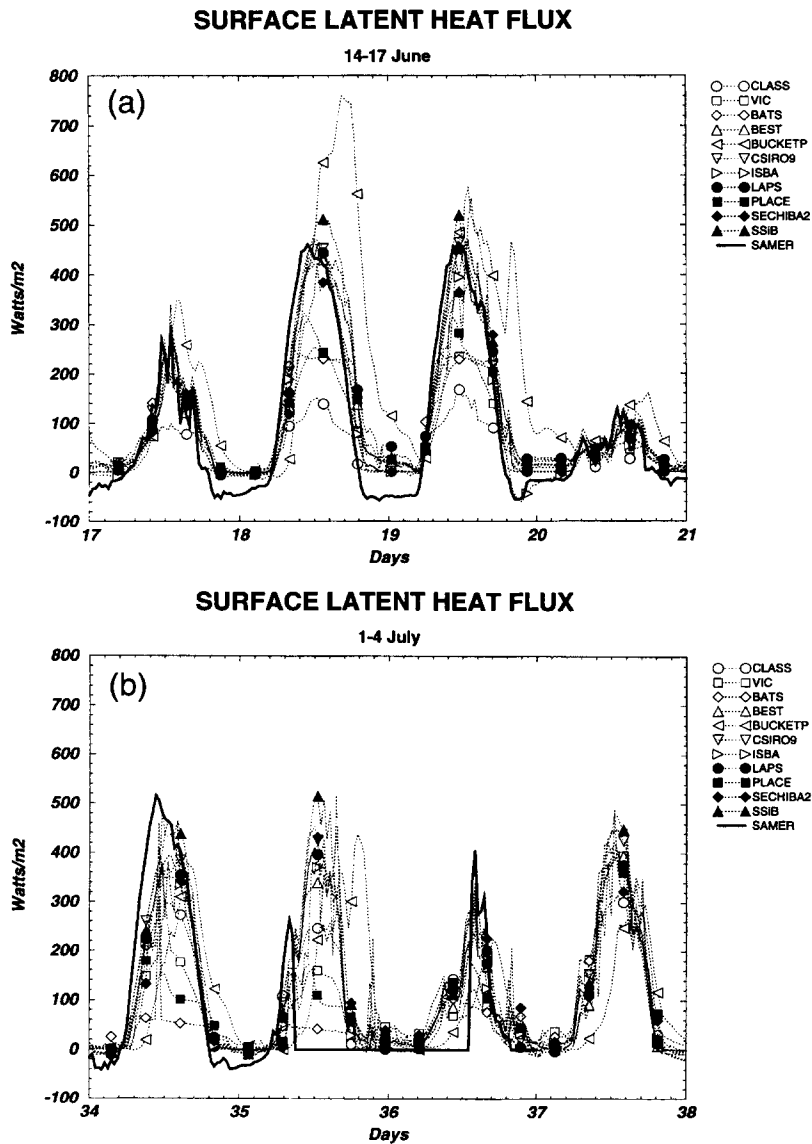


Fig. 3. (a) Observed and predicted values of surface latent heat flux from 14 to 17 June 1986 at Caumont for schemes resolving the diurnal cycle. (b) Observed and predicted values of surface latent heat flux from 1 to 4 July at Caumont for schemes resolving the diurnal cycle.

land surface schemes involved are developed for climate models that resolve the diurnal cycle or for mesoscale models where the time scale of interest is the diurnal cycle. We have selected two 4 day periods in the middle and at the end of the IOP. The first period is chosen around one of the "golden days" of the IOP (16 June); it starts from 14 June and ends on 17 June. Two cloudy situations encompasses two clear sky days where the radiative energy at the surface is high.

Fig. 3a reveals that the BUCKETP model, which was an outlier on the monthly time scale, has a much different behaviour than the other models, because this type of model was not designed to represent the diurnal cycle. The surface latent heat flux is strongly overestimated (up to 300 W/m^2 on the 15 June) and the maximum lags by about 4 hours with respect to observations. During the cloudy days (where the atmospheric demand is low) there is good agreement between the models. However, two models produce a much lower evaporation than the others and observations (CLASS and VIC). Differences are particularly large during the two clear sky days.

Besides the previously mentioned models, two other ones produce a very different diurnal pattern for surface latent heat flux: BATS and PLACE. These models are based on the supply-demand concept for the estimation of the transpiration flux. During the 15–16 June the atmospheric demand is high (net radiation around 600 W/m^2). These models switch at the beginning of the day from an atmospheric demand estimate to a soil-plant supply leading to a plateau around 250 W/m^2 . Other schemes produce a quasi-sinusoidal shape with maxima around 450 W/m^2 in agreement with observations. As observed latent heat is deduced from net radiation it is not surprising to recover the sinusoidal radiative forcing on this quantity. However, it is unlikely that the measured sensible heat could have been underestimated by 200 W/m^2 required to match the models based on supply-demand concept. BEST uses the supply-demand approach but does not show the same behaviour as PLACE and BATS, because that scheme has a larger water holding capacity (the root zone extends over the whole soil depth). The evaporation from SSiB is higher than the other models and than observations. The stress function is inefficient far from the wilting point (due to a depen-

dency in water potential instead of volumetric water content) and soil moisture is rather high.

Examination of another period (1–4 July) reveals identical problems for schemes based on supply-demand approach (Fig. 3b). During 2 July, evaporation produced by BATS is negligible whereas for other models it peaks around 400 W/m^2 . At the end of 3 July an intense convective event occurred filling the water reservoir in the root zone for BATS and PLACE. The day after (clear sky) all the schemes produced high evaporation rates. During dry spells soil moisture depletes progressively reducing the water supply flux. Since schemes like PLACE and BATS have roots only in the first 50 cm of soil, soil moisture can be rapidly depleted with subsequent reduction in transpiration. On the other hand the root zone reservoir can be rapidly wetted by intense rainfall events, leading to more contrasted evaporation regimes than schemes having a bulk root zone (1.6 m). CLASS produces increased evaporation with respect to the previous 4-day period, because it does not have any water stress when soil moisture is above the wilting point. VIC still produces too low evaporation during the first 3 days but agrees with other models when the 50 cm soil layer (root zone) has been partially replenished. Numerical oscillations that appear for SECHIBA2 are linked to the interception reservoir. The peak on evaporation produced by BATS on 1 July is due to evaporation from the interception reservoir when the surface does not limit this quantity. The BUCKETP model still produces too much evaporation after the sunset and too low after sunrise. However, the maxima have been considerably reduced with respect to the previous period. This indicates that BUCKETP switches very rapidly from high to low evaporation rates due to the shape of the β -parameter (Fig. 1).

The comparison over the IOP period shows the BUCKETP model to be an outlier producing too much evaporation. This conclusion is in agreement with previous comparisons of this model versus a more advanced schemes (Sato et al., 1989; Sud et al., 1990). The structure of the vertical layers in the soil, defining the root zone extension, appears to explain some differences between the models, since it gives to a large extent the water holding capacity (the amount of water is available for transpiration). The choices in the values of R_{min} also explain differ-

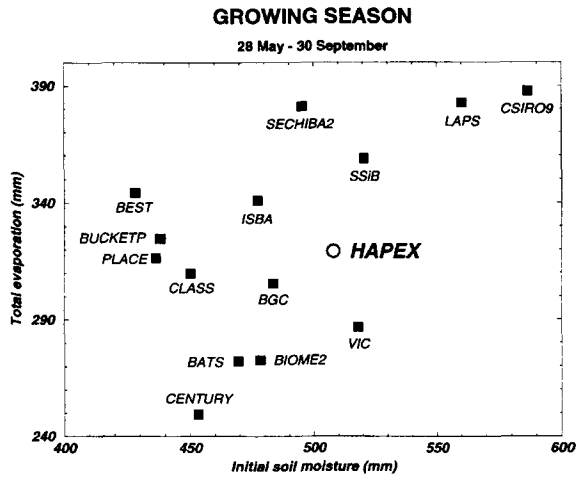


Fig. 4. Scatter plot of initial soil moisture on day 148 (28 May) versus the accumulated evaporation during the growing season (28 May–30 September).

ences in schemes which are conceptually similar. However, ecological designed schemes and atmospheric designed schemes cannot be split into two distinct categories. When associated with a multi-layer soil structure, the supply–demand approach to represent transpiration simulates a diurnal cycle for

latent heat flux incompatible with observations. The problem lies perhaps in an incorrect specification of the extension of roots in the soil, as BEST scheme using the supply–demand concept does not turn off evaporation because of its bulk soil structure in the root zone.

4.2. Growing season (June–September) results

As an attempt to characterize the behaviour of the schemes over the entire growing season (127 days from 28 May to 30 September) in a simple way, two diagnostic variables were assessed: the total soil moisture at the beginning of the growing season, and the cumulative evapotranspiration flux during the growing season. Values were compiled for all schemes from the results of Experiment 13, and the two variables were used as Cartesian coordinates to generate the scatter plot shown in Fig. 4. Reported values of evapotranspiration from the model results were used to generate the cumulative evaporation. This allows examination of the influence of the initial water content at the beginning of the IOP on the total evaporation during the growing season. This may help to sort out problems coming from the

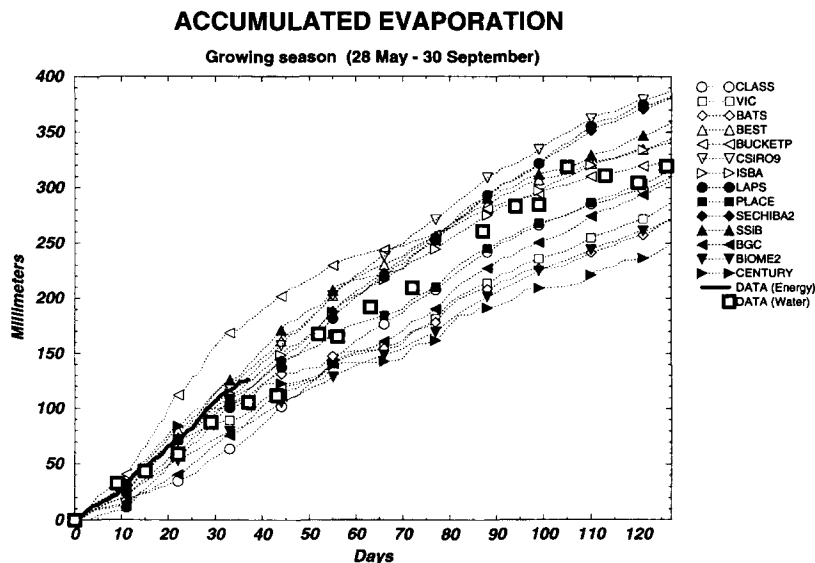


Fig. 5. Observed and predicted values of accumulated evaporation during the growing season of the soya crop at the location of Caumont (from day 148 to day 274). The solid curve corresponds to the atmospheric measurement by the SAMER station (energy balance method) during the IOP and the squares are weekly retrievals from the residual of the surface water balance (soil moisture and precipitation) assuming no drainage.

representation of transpiration from the ones induced by the initial value of soil moisture. Indeed, it is likely that a scheme producing too low evaporation rates or too low drainage in the wintertime period will start the growing season with too high moisture content. In such case, evaporation will be overestimated due to a large extent to excessive water in the soil.

An estimate of the actual growing season cumulative evaporation is derived from the water budget equation, observations of precipitation, observations of total soil moisture, assuming growing season runoff and drainage out of the 1.6 m soil column are negligible.

The surface water budget can be written as (assuming no drainage):

$$\frac{dm}{dt} = P - E$$

where m is the moisture content (in millimeters over the whole soil column), E , the evaporation rate and P , the precipitation rate.

It can be integrated between two times t_1 and t_2 where soil moisture measurements $m(1)$ and $m(2)$ are available, leading to an estimation of the accumulated evaporation during that period of time:

$$\sum E = \int_{t_1}^{t_2} E dt = m(1) - m(2) + \int_{t_1}^{t_2} P dt$$

The assumption of negligible runoff and drainage is supported by observations at the site, reported in Goutorbe et al. (1989), and also 9 of 14 schemes agree that runoff and drainage in this period are small (Table 3). The assumption of zero-runoff allows the inclusion of a point on the scatter plot (Fig. 5) for the observed cumulative evaporation during the growing season. No assumptions are necessary to obtain the soil water at the start of the growing season since it was observed directly.

The schemes can be grouped in three categories corresponding roughly to three of the four quadrants in Fig. 4. Some schemes have a higher moisture content than observed at the beginning of the IOP and evaporate too much during the growing season (CSIRO9, LAPS, SSiB; Group A). The second group also corresponds to schemes having higher accumulated evaporation than observed but for another reason since they start the period with lower soil mois-

ture amounts than observed (SECHIBA2, BEST, ISBA BUCKETP; Group B). These schemes are associated with a single layer in the root zone leading implicitly to a large water holding capacity. In the last category are schemes giving evaporation values lower or close to the observed one (PLACE, CLASS, BGC, BATS, BIOME2, VIC, CENTURY; Group C). All these schemes have a root zone of 50 cm. Some schemes in Group C are located along the first diagonal (BATS, BGC, BIOME2, CENTURY), meaning that those starting with the lowest amounts of soil moisture are producing the lowest total evaporation. This is however not true for VIC, PLACE and CLASS.

The water budget during the growing season (Table 3) shows that one of the three models having too much evaporation produces a non-negligible upward flux of water from the bottom layer (LAPS) which might explain part of its anomalous behaviour. On the opposite VIC and CENTURY simulate a significant drainage flow, that reduces available water for evaporation.

4.3. Comparison of IOP and growing season results

Accumulated evaporation during the whole growing season is depicted on Fig. 5 for the 14 schemes. It also includes both accumulated evaporation measured by the SAMER station during the IOP (previously discussed) and the estimate from neutron probes (integrated soil moisture over the 1.6 m depth) and precipitation (assuming negligible runoff). The model results are spread equally around these observations. Three models produce higher evaporation rates than observed during most of the growing season (SECHIBA2, CSIRO9, LAPS). Four models simulate much lower amounts than reported in the data (CENTURY, BIOME2, BATS, VIC). The shape of the total accumulated evaporation is also instructive. For example, BUCKETP reaches a total amount close to data although considerably overestimating evaporation during the first 50 days. The opposite is true for CLASS where evaporation is underestimated at the beginning but the total cumulative value is correct. For models like BGC, accumulated evaporation is close to a straight line indicating no evidence of water stress at the end the growing phase. On the other hand, for models like BEST, ISBA, CSIRO9

this curve has a bent shape indicating a reduction of transpiration when soil moisture has been sufficiently depleted. Reduction of bare soil evaporation that was rather high for BEST in wintertime is also partially responsible of its behaviour as described in Desborough et al. (1996-this issue). Other models like BATS and CENTURY have a step-like behaviour.

A more precise examination is undertaken over a 40-day period having a strong rainy events (Fig. 6). A 10-day running mean has been done to smooth the curves, and to retain only the long term trend. Schemes with one bulk layer in the root zone (1.6 m) produced high evaporation rates with a rather smooth time evolution (SECHIBA2, BEST, ISBA, BUCKETP). On the other hand, schemes with a multi-layer structure (root zone in the 50 cm top soil layer) lead to periods of low evaporation followed by sharp increases after rainy events (SSiB, CENTURY, BATS, PLACE). BIOME2, VIC and BGC have an intermediate behaviour because they do not have a superficial layer than can fill up rapidly. The difference in water holding capacities means that a given water amount will produce a different effect on transpiration if spread on a 10 cm, 50 cm or 160 cm layer. Unfortunately, daily mean observed values are not available during this period.

4.4. Preliminary conclusions

The previous analysis suggests that part of the differences is related to the structure of the schemes, and part is due to the initial water content at the beginning of the IOP. All three of the ecological models and also BATS and VIC fall in the low evapotranspiration group. Models with a bulk layer in the root zone tend to produce the higher evaporation rates (SECHIBA2, BEST, BUCKETP, ISBA, CSIRO9). The ISBA scheme produces relatively low evaporation in this group due to the high value of minimum canopy resistance chosen. More than half of the models agree with observations during IOP. The only model producing an atypical behaviour is BUCKETP with too high evaporation rates during IOP and too low after that. Moreover, this model produces an unrealistic diurnal cycle of the surface latent heat flux with an important time lag that may come from an overestimation of soil heat capacity. This feature although not new is confirmed by the present study (Sato et al., 1989; Sud et al., 1990). On the daily time scale, the concept of supply–demand used with multi-layer soil models (PLACE, BATS) produces estimates of latent heat flux that do not match observations. Mahfouf and Noilhan (1991)

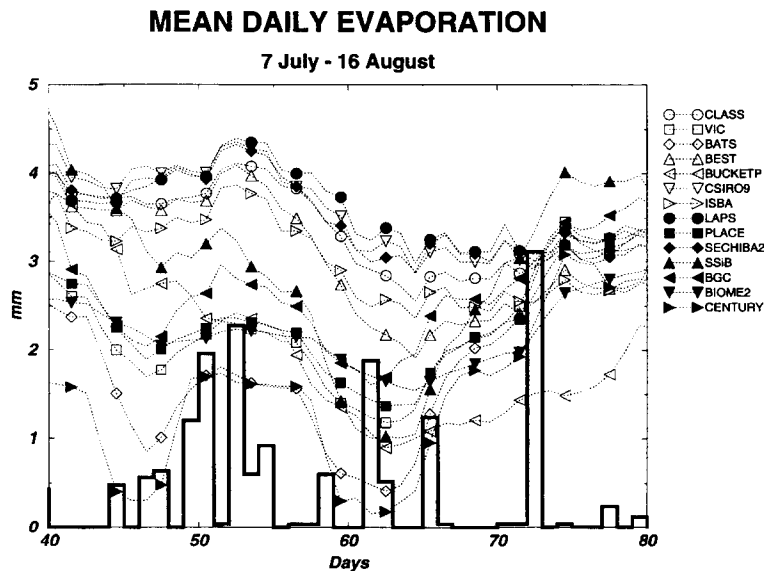


Fig. 6. Mean daily evaporation (10 day running average) from 7 July to 16 August. Daily precipitation is also presented as a thick line to better identify dry and moist periods (units are in mm/5).

have also reported the difficulty for this approach to simulate the diurnal cycle over bare soils. Although the way latent heat flux has been retrieved from measurements links it closely to net radiation, it is unlikely that the very low evaporation rates simulated in dry spells by these schemes are realistic. This highlights the important sensitivity of the supply–demand approach to the specification of the vertical profile of roots within the soil.

5. General conclusions and perspectives

It was clearly demonstrated during the Workshop that the disagreements among schemes in soil moisture prediction, evaporation and sensible heat fluxes are largest during the growing period of the soya crop, caused possibly by profound differences in the treatment of transpiration. Therefore, much attention was paid to trying to understand the variation between models in simulated evapotranspiration and the changes in soil moisture during the growing season. Theory of the transpiration formulations was documented and simulations compared with observations.

The formulations of transpiration are extremely variable between the models represented at the Workshop. Part of this variation is due to fundamental structural differences between models, such as different time-steps or different soil layer structures, and some of it is due to differences in the conceptualization of the transpiration process by the scheme designers. However, stomatal resistance is commonly used to parameterise complicated mechanisms controlling transpiration involving the interaction of abiotic with biotic factors.

After comparing the control experiments with observed HAPEX–MOBILHY data and analysis of additional experiments, it can be concluded that there appear to be two categories of transpiration components in the schemes represented in the Workshop: those falling into the low evapotranspiration group and those in the high evapotranspiration group. It is suggested that these differences are related to the structure of the schemes. However, because of the incomplete nature of the observation data sets, it remains uncertain which of these groups is more likely to be closer to the truth.

The differences between models during the growing season results can be explained as follows:

- The initial moisture content at the beginning of this period resulting from different representations of bare soil evaporation and drainage;
- Relationships between soil moisture and transpiration, and associated tunable parameters (e.g. the minimum stomatal resistance);
- The vertical discretization within the soil producing differences in the amount of water available for transpiration.

The last point is certainly the most crucial, since all schemes having the lowest evaporation rates put the root zone in the top 50 cm of soil because of the chosen vertical discretization (VIC, BIOME2, CENTURY, BATS, BGC) and schemes with a bulk layer including the root zone produce high evaporation rates (ISBA, BUCKETP, SECHIBA2, BEST). SSiB, LAPS and CSIRO9 cannot be split this way because they start in June with too much water in the soil. This aspect certainly explains part of a debate that took place at the beginning of the Workshop about the choice of the wilting point (Experiments 1, 12 and 13). The value of $0.20 \text{ m}^3/\text{m}^3$ for Exp 1 fits the minimum observed soil moisture over the whole soil column. This choice was correct for models having a single layer of 1.5 m in the root zone. However, this value was too high for schemes having roots in the first top 50 cm. In order to increase water holding capacity of multi-layer models, a much lower value has been chosen in experiment 12 ($0.12 \text{ m}^3/\text{m}^3$) and an intermediate one in experiment 13 ($0.15 \text{ m}^3/\text{m}^3$). With these values, multi-layer models match the observed minimum of soil moisture over the whole column, whereas bulk models produce a much lower minimum because of more important water losses. The lack of detailed information about the root system of soya during HAPEX–MOBILHY has prevented us from having a sound specification of water holding capacity. Since such observations will not be available in a foreseeable future at larger scale for which the various schemes are designed, a proper definition of the water holding capacity will remain a problem of landsurface parameterizations for a long time.

Conclusions from this analysis indicate the need for sensitivity experiments to better understand the origin of the differences between the responses of

the land surface schemes during the growing phase of the soya crop. Differences coming from the initial soil moisture can be removed by a 4-month simulation during the growing period starting from the observed soil moisture profile. Sensitivity studies of that kind are already part of the PILPS Phase 1b program.

The HAPEX–MOBILHY dataset has proved to be very useful to evaluate the performance of the land surface schemes over the whole year period in terms of soil moisture evolution. However, in order to go deeper in analyzing the accuracy of the schemes in providing a sound link between soil moisture and evapotranspiration, more consistent datasets are needed. For example, observations of leaf water potential should be made at least as often as the soil moisture measurements. These would provide another validation data set and would allow a more accurate estimation of wilting point and soil pressure–volume curves. Although we recognize that such measurements could not be expected as tuning data sets when the schemes are run operationally, they would provide very valuable information for this sort of comparison project. Important progress has been made during the last ten years in increasing the accuracy of measured surface evaporation over continental surfaces (correction terms for ground heat flux in the energy balance method, eddy-correlation technique). Field experiments following HAPEX–MOBILHY (FIFE 87, HAPEX–SAHEL 92, BOREAS 94) have better documented architectural and biological aspects of plant developments. Moreover, future experiments will be devoted to monitor long term hydrology and will provide useful datasets for improving land surface parameterizations.

Acknowledgements

We would like to thank A. Henderson-Sellers for the initiative of the Workshop. We also acknowledge all the people who contributed to provide the field measurement data from HAPEX–MOBILHY, and particularly P. Peris who processed the one year data of atmospheric forcing. P. Viterbo carefully reviewed the manuscript and provide helpful comments and suggestions.

References

- André, J.C., Goutorbe, J.P., Perrier, A., Becker, F., Bessemoulin, P., Bougeault, P., Brunet, Y., Brutsaert, W., Carlson, T., Cuenca, R., Gash, J., Gelpe, J., Hildebrand, P., Lagouarde, J.P., Lloyd, C., Mahrt, L., Mascart, P., Mazaudier, C., Noilhan, J., Ottlé, C., Payen, M., Phulpin, T., Stull, R., Shuttleworth, J., Schmugge, T., Taconet, O., Tarrieu, C., Thépenier, R.M., Valencogne, C., Vidal-Madjar, D. and Weill, A., 1988. Evaporation over land surfaces: First results from HAPEX–MOBILHY special observing period. *Ann. Geophys.*, 6 (5): 477–492.
- Clapp, R.B. and Hornberger, G.M., 1978. Empirical equations for some soil hydraulic properties. *Water Resour. Res.*, 14: 601–604.
- Cosby, B.J., Hornberger, G.M., Clapp R.B. and Ginn, T.R., 1984. A statistical exploration of the relationships of soil moisture characteristics to the physical properties of soils. *Water Resour. Res.*, 20: 682–690.
- Desborough, C., Pitman, A. and Irannejad, P., 1996. Analysis of the relationship between soil evaporation and soil moisture simulated by 13 land surface schemes for a simple non-vegetated site. *Global Planet. Change*, 13: 47–56.
- Federer, C.A., 1979. A soil–plant–atmosphere model for transpiration and availability of soil water, *Water Resour. Res.*, 15: 555–562.
- Federer, C.A., 1982. Transpirational supply and demand: plant, soil and atmospheric effects evaluated by simulation. *Water Resour. Res.*, 18: 355–362.
- Goutorbe, J.P., 1991. A critical assessment of the SAMER network accuracy. In: Schmugge and Andre (Editors), *Land Surface Evaporation*. Springer, Berlin, pp. 171–182.
- Goutorbe, J.P. and Tarrieu, C., 1991. HAPEX–MOBILHY data base. In: Schmugge and Andre (Editors), *Land Surface Evaporation*. Springer, Berlin, pp. 403–410.
- Goutorbe, J.P., Noilhan, J., Cuenca R. and Valancogne, C., 1989. Soil moisture variations during HAPEX–MOBILHY. *Ann. Geophys.*, 7: 415–426.
- Jarvis, P.G., 1976. The interpretation of the variations in leaf water potential and stomatal conductance found in canopies in the field. *Philos. Trans. R. Soc. London, Ser. B*, 273: 593–610.
- Mahfouf, J.F., 1990. A numerical simulation of the surface water budget during HAPEX–MOBILHY. *Boundary Layer Meteorol.*, 53: 201–222.
- Mahfouf, J.F. and Noilhan, J., 1991. Comparative study of various formulations of evaporation from bare soil using in situ data. *J. Appl. Meteorol.*, 30: 1354–1365.
- Monteith, J.L., 1965. Evaporation and environment. The state and movement of water in living organisms. In: 19th Symp. Soc. Exp. Biol. Academic Press, New York, pp. 204–234.
- Sato, N., Sellers, P.J., Randall, D.A., Schneider, E.K., Shukla, J., Kinter III, J.L., Hou Y.-T. and Albertazzi, E., 1989. Effects of implementing the Simple Biosphere Model in a General Circulation Model. *J. Atmos. Sci.*, 46: 2757–2782.
- Shao, Y. and Henderson-Sellers, A., 1996. Validation of soil moisture simulation in land surface parameterization schemes with HAPEX data. *Global Planet. Change*, 13: 11–46.

- Stull, R.B., 1988. An Introduction to Boundary Layer Meteorology. Kluwer, Dordrecht, 666 pp.
- Sud, Y.C., Sellers, P.J., Mintz, Y., Chou, M.D., Walker, G.K. and Smith, W.E., 1990. Influence of the biosphere on the global circulation and hydrologic cycle: A GCM simulation experiment. *Agric. For. Meteorol.*, 52: 133–188.
- Wetzel, P.J. and Chang, J.-T., 1987. Concerning the relationship between evapotranspiration and soil moisture. *J. Clim. Appl. Meteorol.*, 26: 18–27.
- Wetzel, P.J., Liang, X., Irannejad, P., Boone, A., Noilhan, J., Shao, Y., Skelly, C., Xue, Y. and Yang, Z.L., 1996. Modeling vadose zone liquid water fluxes: Infiltration, runoff, drainage and interflow. *Global Planet. Change*, 13: 57–71.